FUEL EFFECTS ON GAS TURBINE COMBUSTION SYSTEMS

Stanley A. Mosier
Pratt & Whitney Aircraft
Engineering Division
West Palm Beach, FL 33402
USA

SUMMARY

The effects of variations in properties and characteristics of liquid hydrocarbon-base fuels in gas turbine engine combustors was investigated. Baseline fuels consisted of military-specification materials processed from petroleum and shale oil. Experimental fuels were comprised of liquid petroleum blends that were prepared specifically to exhibit desired physical and chemical properties. These fuels were assessed for their influence on ignition and performance characteristics in combustors of the F100, TF30, and J57 (TF33) engines at simulated operating conditions. In general, during relatively short duration tests, combustor ignition and performance became increasingly poorer as fuel quality deviated from specification or historical values.

NOMENCLATURE

B	Mass transfer number in equations (1) and (3)
COP	Combustor operating parameter in equation (2)
FCP	Fuel characterization parameter in equation (3)
FPR	Fuel characterization parameter ratio in equation (4)
LSP	Liner severity parameter in equation (7)
PF	Pattern factor in equation (5)
Pr_a	Prandtl number of air in equation (2)
RDS	Relative droplet size in equation (1)
ref	Reference, or referee
SG	Specific gravity in equation (1)
SMD	Sauter mean diameter in equations (1) and (3)
Spec	Specification
Tu	Percent turbulence intensity in equation (2)
U	Free-stream air velocity in equation (2)
VI	Vaporization index in equation (1)
ϕ	Equivalence ratio
ρ_a	Density of air in equation (2)
ρ_f	Density of fuel in equation (3)
μ_a	Dynamic viscosity of air equation (2)

1. INTRODUCTION

Gas turbine engines for military aircraft have been designed and developed historically to operate on high-quality, liquid hydrocarbon fuels produced to very exacting specifications. These specifications were formulated as a compromise between desired performance characteristics of the fuel and the concurrence of the processor to supply the quantities of fuel needed at an acceptable price using available technology. The specifications were composed at a time when crude oil was plentiful and cheap. Consequently, values of selected physical and chemical properties were chosen that were sufficiently conservative to fully accommodate the most extreme environmental conditions under which current and future turbine-powered military aircraft might operate. In 1973, before the oil embargo, refiners were supplying high-quality jet fuel to the military services for approximately eleven cents per gallon; the Air Force's bill at that time for 143 million barrels of turbine-engine fuel was less than 600 million dollars (Reference 1).

The specifications established in the pre-embargo era essentially committed operational aircraft engines and those both under development and on the drawing boards to use high-quality fuel during their lifetimes. Because of the ready availability of such fuel at that time, the specifications were not optimized using sensitivity tradeoffs relating the values of key fuel properties to the operation and

performance of engine components and systems. Few such tradeoff studies had either been conducted or documented. As a consequence, there is concern that in the light of today's economic and energy situations, the established fuel specifications might be too rigid: possibly limiting the availability of the jet-fuel supply and contributing to its high cost. In 1982, the price of a gallon of jet fuel supplied to the Air Force had been escalated to $1.30; the annual bill for the 95 million barrels used was over five-billion dollars (Reference 2). There is also concern that portions of the specification might be too loose and need to be made more restrictive; this type of change might again tend to limit fuel availability and increase its price.

Consequently, for several years the Department of Defense has been sponsoring fuel-accommodation investigations with gas turbine engine manufacturers and supporting organizations to quantify the effect of changes in fuel properties and characteristics on the operation and performance of military engine components and systems. Inasmuch as there are major differences in hardware, between the operational engines in the Air Force and Navy inventories, due to differences in design philosophy and requirements, efforts were initially expended to acquire fuel-effects data from rigs simulsting the hot-sections of these different engines. Correlations were then sought using the data acquired to produce more general, generic relationships that could be applied to all military gas turbine engines regardless of their origin. Finally, models could be developed from these correlations that could predict the effect of fuel property changes on current and future engines.

This paper describes some of the work performed by Pratt & Whitney Aircraft under Defense Department-sponsored fuel-effects programs. The experimental work was conducted using hot-section components from the F100, TF30, and TF33 engines. The analytical effort incorporated data obtained from tests of these components as well as data obtained by other investigators from rig tests of their engine hot-section components. Reference has been made in the text to contractor reports in which the experimental results and data cited in this paper have been taken.

2. TEST PROGRAMS

Two test and evaluation programs were conducted to determine the impact of jet fuel property variations on the ignition and performance/durability characteristics of three combustion systems used in current operational military aircraft. One investigation addressed the F100 engine, which is used in the Air Force's F-15 and F-16 aircraft, and the TF33 engine, which is used in the Air Force's B-52H, C-135B, C-141 and E-3A aircraft. The other investigation addressed the TF30 engine that is used in the Navy's F-14 aircraft. Both programs were performed using test rigs comprised of engine combustion system hardware.

Tests were conducted at conditions that closely simulated those of the three engines under investigation using the experimental fuels that are described later. Ignition tests were conducted for both sea-level (groundstart) and altitude (airstart) operation over a range of fuel temperatures. For the airstart test program, simulated altitude conditions were selected from windmilling maps of each engine; these maps are shown in References 3-6. Performance tests were conducted at four simulated power settings. Rig test conditions are shown in Table 1. For the F100 and TF30 rigs these settings corresponded to idle, cruise, takeoff and dash. For the TF33 rig, the settings corresponded to idle, takeoff, and two cruise conditions; a second cruise condition was substituted for the high-altitude dash because the TF33 is not used in fighter applications.

Table 1. Nominal Operating Conditions for Performance/Durability Rig Tests

Rig	Condition	Inlet Air Temp, K	Inlet Air Press, kPa	Inlet Airflow Rate, kg/s
TF30	Idle	440	370	2
	Takeoff	750	1790	6
	Cruise	620	900	3
	Dash	790	1560	5
F100	Idle	490	450	4
	Takeoff	700	1160	8
	Cruise	810	1470	10
	Dash	900	1480	10
TF33	Idle	360	210	2
	Takeoff	550	430	4
	Cruise 1	600	530	4
	Cruise 2	660	1260	10

3. COMBUSTOR HARDWARE

Five mainburner test rigs were used in conducting the experimental programs. A 90-degree sector rig was used for determining both ignition and performance characteristics of the F100 combustor. Full sets of cans, in annular arrangements, were used for ignition testing of the TF33 and TF30 combustors; performance testing was accomplished using single cans.

The F100 burner rig consisted of a diffuser case, an instrumented combustor, and four, engine-quality airblast fuel injectors. The rig was fabricated by cutting the appropriate sector from an engine diffuser case and combustor and attaching louver-cooled sidewalls to both. The engine burner is shown schematically, in cross section, in Figure 1. The liner was instrumented with chromel-alumel thermocouples distributed axially and circumferentially to acquire temperature gradient data for estimating combustor liner life. A detailed description of the rig is provided in Reference 4.

Two rigs were used in the TF33 test program. The ignition rig was comprised of eight cans joined together with dome-located cross-over tubes in an annular arrangement within an engine case; each combustor was equipped with six pressure-atomizing fuel injectors. Engine igniters driven by engine exciter boxes supplied the energy and spark rate for ignition to two of the cans. The performance rig consisted of a single instrumented can, equipped with fuel injectors, mounted in a containment vessel that simulated a 45-degree segment of the engine case; and an inlet duct and transition duct constructed from actual engine hardware. The combustor can, shown in Figure 2, was instrumented with thermocouples and small-diameter tubes to obtain liner temperatures and static pressures, respectively. The combustor rigs are described in detail in Reference 4.

Two rigs were also used in the TF30 test program. The ignition rig was comprised of eight interconnected cans in an annular arrangement within an engine case; each combustor was equipped with four pressure-atomizing fuel injectors. Two of the cans were adapted with engine igniters driven by exciter boxes that simulated the energy and spark rate of the engine system. The performance rig, shown in Figure 3, consisted of a single instrumented can equipped with fuel injectors, mounted in a case, with inlet and transistion ducts, simulating one-eighth of the full-annular flowpath of the engine. The combustor liner and transition duct were instrumented with thermocouples to obtain information from which liner life could be estimated. In addition, the can and transition duct were fitted with small-diameter tubes for obtaining liner static pressure measurements. The combustor rigs are described in detail in References 3 and 5.

4. TEST FUELS

A total of 21 liquid hydrocarbon fuels in three categories were selected for use in the fuel-effects programs. The first category was comprised of jet fuels made to military specifications from both petroleum and shale oil. These served as referee fuels primarily to establish baseline values of combustor operating characteristics. The second category consisted of two sets of nonspecification fuels produced from petroleum. These fuels were blends of refinery streams that were proportioned to exhibit pronounced variations in values of selected properties. The properties addressed were those that were predicted to most significantly influence combustor ignition and performance. The third category included blended fuels that were prepared primarily to represent reduced-quality petroleum refinery products or emergency fuels. These were incorporated into the programs primarily for their holistic impact.

Six fuels were included in the first category. Two were produced to JP-4 specifications and four were made to JP-5 specifications. One of the JP-4 fuels and one of the JP-5 fuels were prepared from oil shale; the remainder were prepared from petroleum. Representative properties of the referee fuels are shown in Table 2 relative to JP-4 and JP-5 specification values; detailed property information is provided in References 3-6.

Table 2. Selected Properties of Referee Fuels

Fuel Reference No. Fuel Type	2-1 JP-4 (Spec.)	2-2 JP-4	2-3 JP-4 (Shale)	2-4 JP-5 (Spec.)	2-5 JP-5	2-6 JP-5	2-7 JP-5	2-8 JP-5 (Shale)
Hydrogen Content, % wt	13.6*	14.54	14.39	13.5*	13.93	13.79	13.81	13.85
Aromatics Content, % vol	25.0**	11.1	10.1	25.0**	15.9	15.8	22.6	24.0
Viscosity, mm^2/s	-	0.97(294K)	1.28(294K)	8.5(253K)**	2.29(289K)	1.58(311K)	2.04(289K)	2.00(289K)
Specific Gravity at 288K	0.751-0.802	0.760	0.781	0.788-0.845	0.815	0.817	0.809	0.807
Initial Boiling Point, K	-	293	273	-	431	454	450	459
10% Recovery Temp, K	-	358	400	478**	470	472	466	467
20% Recovery Temp, K	418**	374	421	-	474		471	469
50% Recovery Temp, K	463**	431	458	-	489		482	480
90% Recovery Temp, K	518**	495	500	-	516	516	509	505
End Point, K	543**	589	593	563**	535	534	529	527
Freezing Point, K	215**	214	214	227**	227	223	227	227
Flash Point, K	-			333*	338	335	339	339
Heat of Combustion, MJ/kg	42.8*	43.401	43.469	42.6*	43.260	43.041	43.100	43.144

* Minimum acceptable values
** Maximum acceptable values
\- No value specified

The second category consisted of eight fuel blends in two sets. The first set contained four fuels that were selected to exhibit parametric variations in those properties indicated to impact ignition characteristics most significantly. The properties of primary interest in the preparation of these ignition fuels were viscosity and volatility. Three of the fuel blends were produced to exhibit

specified variations in these two properties, including one blend for evaluating the significance of the shape of the front end of the distillation curve. The fourth fuel was selected for evaluating chemical effects, related to aromatic structure, on ignition characteristics. The second set of four fuels was produced to evaluate the sensitivity of combustor performance characteristics to variations in fuel properties. These characteristics included pattern factor, liner durability, exhaust gas objectionable emission concentrations, and combustion efficiency at low-power operation. Key properties operated on to produce the performance fuel blends were viscosity, aromatics content and type, hydrogen content, and volatility. Pertinent properties of the ignition and performance fuels are shown in Table 3. Properties of the seven blending stocks that were used in preparing the test fuels, as well as detailed characteristics of the test fuels, are provided in Reference 4.

Table 3. Selected Properties of Ignition and Performance Fuels

	Ignition Fuels				Performance Fuels			
Fuel Reference No.	3-1	3-2	3-3	3-4	3-5	3-6	3-7	3-8
Hydrogen Content, % wt	14.24	13.44	14.04	12.27	13.44	12.94	11.56	11.50
Aromatics Content, % vol	10.5	27.5	13.8	55.4	20.1	34.7	61.6	45.5
Naphthalene Content, % vol	2.1	0.7	0.7	0.4	2.8	3.8	4.0	14.9
Viscosity, mm^2/s								
239K	Solid	3.46	6.74	1.73	8.11	5.60	18.8	Solid
244K	5.56	3.03	5.68	1.50	6.56	4.25	12.6	Solid
273K	2.55	1.66	2.55	0.96	2.83	2.09	4.34	4.93
294K	1.71	1.17	1.71	0.74	1.87	1.46	2.65	2.85
311K	1.33	0.94	1.32	0.62	1.42	1.16	1.93	2.03
T (K) at % Recovered								
10	370	395	459	365	432	368	430	470
20	399	422	462	384	452	394	435	481
50	509	456	473	419	482	461	483	522
90	542	499	494	442	522	575	611	581
Specific Gravity at 288K	0.789	0.796	0.801	0.795	0.817	0.814	0.879	0.886
Freezing Point, K	244	216	225	204	226	239	235	253
Flash Point, K			315		319		313	336
Heat of Combustion, MJ/kg	43.287	43.001	43.232	42.560	42.818	42.537	41.212	41.451

The third category was comprised of seven petroleum-base blends. Four were prepared from refinery streams to be representative of production-type, relaxed-specification jet fuels. The remaining three were selected to be representative of emergency fuels. One of the emergency fuels was a No. 2 fuel oil; the other two were blends of nonaviation fuels and specification-grade JP-5. Some of the principal properties of these fuels are shown in Table 4. Detailed physical and chemical properties of these fuels are provided in Reference 5.

Table 4. Selected Properties of Relaxed-Specification/Emergency Fuels

	Relaxed-Specification Fuels				Emergency Fuels		
Fuel Reference No.	4-1	4-2	4-3	4-4	4-5*	4-6**	4-7***
Hydrogen Content, % wt	13.36	13.48	13.66	13.82	13.22	12.83	13.54
Aromatics Content, % vol	28.5	19.8	22.8	18.6	25.9	26.4	18.6
Viscosity, mm^2/s at 311K	1.78	2.27	1.62	1.74	2.60	1.77	2.06
Specific Gravity at 288K	0.830	0.836	0.819	0.817	0.839	0.847	0.830
Initial Boiling Point, K	436	441	444	453	426	466	453
10% Recovery Temp, K	463	500	465	475	491	477	477
90% Recovery Temp, K	549	545	534	537	590	545	570
End Point, K	570	554	549	555	606	561	596
Freezing Point, K	243	249	239	239	270	242	263
Heat of Combustion, MJ/kg	42.648	42.798	42.919	42.961	42.706	42.392	42.873
Flash Point, K	330	344	332	342	346	344	349

* No. 2 fuel oil
** 20% (vol) hydrocracked gas oil + 80% (vol) JP-5
*** 50% (vol) Diesel Fuel Marine + 50% (vol) JP-5

For ease of identifying the various test fuels throughout the test, all of the fuels in the three tables have been assigned two-digit reference numbers. The first digit refers to the table number and the second digit to the reference number of the fuel in the table. For example, the shale-base JP-5 referee fuel in Table 2 is Fuel 2-8, and the emergency fuel comprised of Diesel Fuel Marine and JP-5 is Fuel 4-7.

5. TEST RESULTS

A significant amount of experimental data was obtained during the conduct of the fuel-effects programs. No attempt will be made in this paper, however, to present all of the data acquired for the combustor rigs and 21 fuels investigated; this information is contained in contractor final reports (References 3-6). The objective of this paper is to provide a condensation of these reports, supplying representative results from the ignition and performance investigations. These results include both input - output information and correlations depicting fuel-property effects on combustor rig characteristics.

(a) GROUNDSTART IGNITION

Groundstart ignition testing was conducted over a range of airflow rates to determine the minimum fuel flow at which stable ignition could be achieved in a given combustor rig. For the can-annular arrangements, stable ignition was considered attained when all combustors lit within 30 seconds after fuel flow had been initiated. For the sector burner, stable ignition was considered achieved if burning was observed directly downstream of each of the four injectors within 30 seconds of fuel initiation. Prior to each ignition attempt, a common temperature was established for the inlet air, fuel, and test rig.

The data shown in Figure 4 are representative of those obtained during groundstart ignition testing. In this figure, results for the F100 sector burner rig are presented for a simulated cold day (244K) using the two baseline JP-4 fuels (Table 2) and the four ignition fuel blends characterized in Table 3. In general, petroleum-base JP-4 fuel lit at the lowest flowrates. The other fuel blends, and the shale-base JP-4 fuel, lit at higher flowrates. The increases were essentially proportional to the relative droplet size (RDS) of the fuel, i.e. the ratio of the Sauter mean diameter achieved for the fuel under investigation, using a given injector, to the Sauter mean diameter obtained for a baseline fuel when the same injector is used; and the fuel volatility, as represented by the 10% recovery temperature. As the relative droplet size of the test fuel increased, due to higher values of viscosity, surface tension, and density, and as the 10% recovery temperature increased, a higher fuel flowrate, indicative of a higher fuel-air ratio, was needed to effect groundstart ignition.

Figure 5 shows the results of a more general correlation that was developed for predicting groundstart ignition characteristics. In this case, the combustor was the TF30 and the fuels used were the referee low-aromatic content JP-5 fuel, identified in Table 2 as Fuel No. 2-6, and five of the fuels identified in Table 4. The fuel-air ratio required for full rig ignition at each of three airflow rates is presented as a function of a vaporization index, which is defined in equation (1).

$$VI = \frac{(RDS)^2(SG)}{\log (1 + B)} \qquad (1)$$

This equation,described in more detail in the Appendix, contains physical properties of the fuel both explicitely, as specific gravity (SG) and implicitely through relationships defining relative droplet size (RDS) and mass transfer number (B). As the index increases, there is less propensity for the fuel to ignite at any given value of airflow rate. Higher values of the index represent heavier, poorer-quality fuels having, inter alia, higher densities, surface tensions, and viscosities and lower volatility characteristics. In this case, characteristics of heavier, poorer-quality fuels were also achieved by reducing the temperatures of three of the test fuels.

(b) AIRSTART IGNITION

Airstart ignition tests were conducted to determine the capability of each of the three combustor rigs to achieve stable ignition at simulated altitude conditions using a variety of test fuels. Stable ignition in these tests was defined as it was for groundstart ignition. Altitude conditions simulated for these tests were selected from standard-day windmilling maps. These maps represent known windmilling operating regions within the bounds of aircraft altitude and Mach number for the engine combustors under investigation. The aerodynamic variables involved include flowrate, total pressure, and temperature of the air entering the combustor rig; flight Mach number, and altitude. By specifying any two of these variables, the others can be obtained from the windmilling map for the engine.

The fuel-dependent variables include physical and chemical characteristics of the blends being introduced into the rig, and the fluid dynamical factors that determine the characteristics of the fuel-air mixture in the vicinity of the igniter. In general, as the quality of the test fuel deteriorated, as indicated by increased viscosity and surface tension, and decreased volatility, the capability of a combustor rig to ignite stably at simulated altitude conditions decreased. Figure 6 is representative of the impact of fuel properties on airstart ignition for the TF30 combustor rig at a temperature of 40 F (278K). The fuels used were a referee JP-5 that was described in Table 2 (Fuel No. 2-6), and five of the broadened-specification and emergency fuels described in Table 4. The referee JP-5 fuel and the emergency fuel blend (comprised of Diesel Fuel Marine and JP-5) clearly provided the best and worst airstart ignition characteristics, respectively. Performance of the other fuels lay essentially midway between the two extremes.

The capability of a combustor rig to ignite stably also decreased when the temperature of the fuel, inlet air, and rig were reduced. In a sense, the fuel viscosity, surface tension, and volatility were degraded artificially to simulate characteristics of poorer-quality fuels. Figure 7 shows the variation in airstart ignition capability with temperature for a TF30 mainburner rig fired with the

referee JP-5 fuel (No. 2-6) that was described in Table 2. The impact of increasing viscosity and surface tension, and lowering volatility on airstart ignition characteristics is as pronounced as if poorer quality fuels were used.

Airstart ignition results as presented in Figures 6 and 7 faithfully represent rig characteristics for the fuels investigated. However, fuel property influences are not in a form that would enable the degradation in altitude ignition capability with fuel properties to be readily ascertained. Consequently, a model was formulated and a correlation developed that did, indeed, allow this to be accomplished. The model is based on the work of Ballal and Lefebvre (Reference 7) and on the observation that over a wide range of combustor aerothermal operating parameters, the ignition process is evaporation-rate controlled. It is assumed that a spark creates a spherical volume of inflamed gas that, if it is to propagate through the gas mixture, must be of sufficient size that the rate of heat release within its volume exceeds the heat loss to the surroundings. The radius of the critical volume is termed the quenching distance and the energy required is the minimum ignition energy.

For a given combustor design the quenching distance and, hence, the required energy are functions of the aerodynamic conditions within the combustor, the fuel droplet diameter, and the fuel volatility. The internal combustor aerodynamics are directly related to flight conditions, viz. altitude and Mach number. The droplet size is determined by injector characteristics and by the fuel viscosity, density, and surface tension. The energy liberated by the igniter varies slightly with the aerothermal condition, but may be assumed to be constant over the range considered. Therefore, the quenching distance can be taken as a measure of ignition capability.

The relationship developed by Ballal and Lefebvre (Reference 7) for the quenching distance, was rewritten to isolate terms dependent on combustor aerodynamics from those dependent only on the fuel. The aerodynamic grouping, containing terms that vary with altitude and Mach number, is referred to as the combustor operating parameter, COP, and is defined as

$$COP = \frac{Pr_a}{10\phi}\left[\frac{Tu\ U}{\rho_a\ \mu_a}\right]^{0.5} \qquad (2)$$

The fuel-dependent variables are collected in the fuel characterization, or correlation, parameter, FCP, which is defined as

$$FCP = \frac{\rho_f (SMD)^{1.5}}{\log\ (1 + B)} \qquad (3)$$

The combustor operating parameter can be calculated from operating conditions defined on a windmilling map for the engine in question. Figure 8 shows the variation in altitude with combustor operating parameter for a TF30 combustor rig.

To the extent that the ignition scenario and model are valid, there is a fixed relationship between the values of the combustor operating parameter and the fuel characterization parameter that will result in ignition. Figure 9 shows such a relationship that was developed from airstart ignition data for the TF30 combustor rig using three of the referee fuels identified in Table 2. The fuels were a low-aromatic content JP-5 (Fuel No. 2-5), a high aromatic JP-5 (Fuel No. 2-7), and a shale-base JP-5 (Fuel No. 2-8). The data indicate a linear relationship between the two parameters for each of the four burner airflow rates investigated. For a particular airflow rate, any combination of the two parameters falling below the correlation line for a specific airflow rate would indicate a "no-light" situation; any combination falling on or above the line would indicate stable-ignition.

Figures 8 and 9 in combination form a basis for predicting the effect of fuel changes on airstart capability. For a given fuel, the fuel characterization parameter is first calculated from fuel properties and injector characteristics. For this value of the fuel characterization parameter, the ignition limit of the combustor operating parameter is then defined by Figure 9 at each airflow rate. Finally, the value of the combustor operating parameter is converted to altitude using Figure 8.

A refinement of the preceding model was formulated to provide a simplified airstart ignition correlation. Using Figure 8, with a referee JP-5 fuel as the baseline, the change in value of relight altitude between that resulting from the use of the referee fuel and that resulting from the use of the test fuel was determined as a function of the fuel characterization parameter for each of the four airflow rates. Each fuel characterization parameter was then normalized, using the fuel characterization parameter for the referee JP-5 fuel, to obtain a fuel characterization parameter ratio, FPR, which is defined in equation (4).

$$FPR = \frac{FCP}{(FCP)_{JP\text{-}5}} \qquad (4)$$

The resulting plot is shown in Figure 10, where the difference in relight altitude for the TF30 combustor rig is presented as a function of fuel properties and airflow rates. Fuels having ignition qualities better than those of the referee military-specification fuel are identified by fuel parameter ratios less than unity, increases in relight altitude above that of the referee fuel are identified by fuel parameter ratios greater than unity.

The validity of the approach taken to produce Figure 10 was tested using data from airstart ignition tests in which a number of the fuels listed in Table 4 were evaluated. As discussed earlier, the fuels in Table 4 were prepared to be fully representative of relaxed-specification and emergency fuels. Figure 11 presents the results obtained for the specified test fuels relative to the 27,000 lb/hr (3.4 kg/s) airflow rate correlation line shown in Figure 10. The good correlation achieved for this airflow rate line was also obtained for the remaining three airflow rate lines.

(c) PATTERN FACTOR

Pattern factor, PF, defined in equation (5), was determined from temperature measurements of the air entering the performance combustor rig and of the working fluid leaving the rig.

$$PF = \frac{T_{max,out} - T_{avg,out}}{T_{avg,out} - T_{avg,in}} \qquad (5)$$

where $T_{max,out}$ = maximum exhaust gas temperature measured in the plane of the turbine first-stage vane

$T_{avg,out}$ = average temperature of the exhaust gas in the same plane

$T_{avg,in}$ = average temperature of the combustor inlet air

This parameter provides a measure of the quality of the working fluid being supplied by the combustor to the turbine, which influences turbine durability and performance. The lower the pattern factor, the greater the durability of the turbine.

The best means of determining pattern factor for an engine is by using the engine itself as the test bed. In this way, the influences of combustor inlet air distribution, associated with a specific compression system, and internal aerodynamics, resulting from the interaction of the fuel and air injection systems, are measurable exactly. Unfortunately, this type of testing is not routinely possible because of the high costs of preparing for and conducting the tests. In the case of determining the effect of fuel properties on hot-section performance, engine hardware could be jeopardized because of the many unknowns involved. Therefore, although engine testing would provide the best data on fuel-dependent pattern factor effects, combustor rigs, with their inherent deficiencies, were used to develop relative trends. From these trends, however, the magnitude of fuel effects on engine hardware can be projected and then engine testing, incorporating automated recording temperature systems (ARTS) in the first turbine vanes, could be indicated to quantify the rig trends and refine the preliminary models and correlations.

The trends obtained in pattern factor variations with fuel properties were found to correlate, generally, with the vaporization index of the fuel, which was defined in equation (1). However, in the performance-test version of this index, the 90% recovery temperature of the fuel, was used in determining the relative droplet size and mass-transfer number. Processes within the combuator that would tend to influence droplet size, penetration, and evaporization and then impact pattern factor were considered to be more dependent upon the final stages of droplet life than upon the initial stages.

Figure 12 shows a correlation indicating the influence of fuel properties on pattern factor and, in turn, their impact on the predicted low-cycle fatigue life of a first-stage turbine vane for the TF30. The data have been normalized to emphasize trends rather than absolute values, which for this type of rig testing are of little value. As the pattern factor increases, the low-cycle fatigue life is predicted to decrease as would be expected. However, the impact of fuel properties on pattern factor, both explicitly in terms of hydrogen content of the fuel and implicitly through vaporization index, are well depicted. Although the magnitude of the trends observed are not especially pronounced, the potential impact on turbine life due to the fuel burned is significant. As fuel quality deteriorates in terms of viscosity and volatility, the resulting turbine performance, in terms of durability, is projected to deteriorate.

(d) LINER DURABILITY

The life of conventionally cooled combustor liners in operational aircraft engines is generally limited by cracks in specific louver seam welds caused by low-cycle fatigue. Low-cycle fatigue results from cyclic expansion and contraction of the combustor liner during engine operation. Crack initiation occurs at locations in the liner where high stresses exist due to severe thermal gradients. This location is usually at a seam weld between two adjacent louvers, as shown in Figure 13, where a relatively large temperature gradient exists between the louver wall and the knuckle. At high-power operating conditions the stress concentrations in the vicinity of the seam weld can be well above the yield strength of the material causing plastic deformation with each cycle.

For a specific engine operating condition at which a referee fuel is burned, a thermal gradient is established between the louver lip and the knuckle causing a bending stress in the seam weld. When a poorer quality fuel is substituted for the referee fuel and is burned, the flame luminosity increases, which increases the temperature of the louver lip, but not the colder knuckle. The knuckle temperature remains essentially constant because of the radiation shielding provided by the lip and the temperature invariance of the cooling air entering the vicinity of the knuckle. Consequently, the increased flame luminosity increases the lip-to-knuckle thermal gradient and causes higher stresses in the seam weld.

Estimates of relative liner life were made for the F100 and TF30 combustors using measured liner temperatures from tests in which both baseline and experimental fuels were burned. To ensure the achievement of maximum strain in the critical louvers of the liners, the Type I engine cycle (off to max to off) was used to estimate fuel effects on F100 combustor life, and the Type I and Type II engine cycles (off to max to off with Type II going to supersonic) for the TF30 estimates.

The technique used for the low-cycle fatigue snalysis incorporated equation (6) for calculating thermal strains.

$$\frac{\Delta\epsilon_T}{\Delta\epsilon_{baseline}} = \frac{\Delta T_T}{\Delta T_{baseline}} \tag{6}$$

where $\Delta\epsilon_T$ = total strain from burning the test fuel

$\Delta\epsilon_{baseline}$ = total strain from burning the baseline fuel

ΔT_T = temperature differential between seam weld and knuckle when test fuel is burned

$\Delta T_{baseline}$ = temperature differential between seam weld and knuckle when baseline fuel is burned

A value of baseline strain was taken from a figure relating the dependence of total strain range on cycles to failure for the liner material over a range of metal temperatures. Field history provided information on cycles to failures for the engine combustors.

Figure 14 shows the variations in life for the F100 and TF30 combustors that were estimated using rig temperature data, equation (6), and the low-cycle fatigue properties of the liner materials as a function of the hydrogen content of the fuel burned. The abscissa has been normalized by the hydrogen contents of the baseline fuels used in the test programs for the two combustors. Also shown in figure 14 are variations in predicted combustor liner life with the fuel hydrogen content parameter for two models of the J79 engine (Reference 8) and for the F101 (Reference 9). All trends are generally the same; as the hydrogen content of the fuel is reduced, the predicted liner life is also reduced. The magnitude of the predicted reductions in life are dependent upon the strain model selected, the materials data used, and the baseline information from field experience.

During the conduct of the TF30 fuel-effects investigation, a porous-plug radiometer was installed in the liner to measure the radiative heat load from the burning of lower-quality fuels. Figure 15 shows the variation in measured radiative heat flux with the hydrogen content of the fuel being burned at a number of operating conditions. As expected, the thermal radiation contribution to the total heat transfer rate from the combustion process to the liner increased as the hydrogen content of the fuel decreased. The significance of the increased thermal radiation load on combustor liner life at sea-level takeoff conditions is shown in Figure 16. For a seven percent decrease in hydrogen content of the fuel, the radiant heat flux increased by 16 percent resulting in a predicted reduction in liner life of approximately ten percent.

Combustor liner metal temperatures measured in the test programs and used in the durability analyses were correlated using a liner severity parameter, LSP, which is defined in equation (7).

$$LSP = \frac{T_{metal,max} - T_{air,in}}{T_{gas,out} - T_{air,in}} \tag{7}$$

This parameter is similar in form to that for pattern factor, equation (5). When plotted against the hydrogen content of the fuel burned, the liner severity parameter indicates the sensitivity of liner hot-spot temperature to poorer quality fuels. As shown in Figure 17 for a variety of combustor rigs operating at sea-level takeoff conditions, as the hydrogen content of the fuel being burned was decreased, the liner severity parameter increased. Although the rate of change of this parameter to hydrogen content was relatively small for all of the combustors considered, the magnitude of the parameter differed significantly for each.

(a) COMBUSTION EFFICIENCY

The combustion efficiency for a gas turbine combustor is a measure of the effectiveness in which chemical reactions between fuel and air are completed within a given volume. This effectiveness is strongly dependent upon the preperation of the fuel-air mixture. Under high-power conditions, the fuel injectors operate in a range where atomization is optimum and rapid veporization of the injected fuel is enhanced by high temperatures of the inlet air. At low-power operating conditions, atomization is generally poorer, resulting in larger droplets being injected; and inlet air temperatures are lower, resulting in less of the incoming fuel being vaporized.

Poorer preparation of the fuel-air mixture for reaction contributes to an observed lower combustion efficiency at idle: especially with those engines having low pressure ratios. Intrinsic in the variables effecting fuel preparation are the physical properties of the fuel. Higher values of viscosity and surface tension, and lower values of volatility can yield larger, less vaporization-prone droplets.

The effect of fuel properties on combustion efficiency at the idle power setting was examined using data acquired in the F100, TF33 and TF30 burner investigations (References 3-6). Date obtained from other sources were also examined to obtain fuel-dependency comparisons between different combustion systems (References 10-13). The correlating parameter selected for combustion efficiency at the idle power setting is the veporization index, which was defined earlier in equation (1). It is conjectured that idle efficiency is controlled by the ability of the final portion of the fuel spray (the portion associated with the upper end of the distillation curve) to vaporize rapidly enough to react before leaving the combustor. For this reason the mass transfer number in the denominator of equation (1) was

evaluated at the 90% recovery temperature for each fuel investigated. As described in an earlier section, as the value of the vaporization index increases, the tendency for the fuel to vaporize decreases. The poorer preparation of the fuel-air mixture contributes to a lower value of combustion efficiency being obtained.

The vaporization index for each of the fuels tested in a given combustor was normalized by the value of the vaporization index for that combustor when a referee fuel was burned. Likewise, the value of combustion efficiency at idle power operation for each fuel was normalized using the efficiency measured for the combustor in question when the same referee fuel was burned. Consequently, the fuel effect trends, relative to conventional, military-specification fuels, can be more readily ascertained. In addition, this technique provided a means to compare the fuel-effects trends for all combustors on a common basis.

Figure 18 shows the resulting variation in idle efficiency ratio with vaporization index ratio for rigs representative of combustors in the F100, TF33 and J79 engines. These systems were selected as being typical of high pressure ratio modern powerplants and of more mature, lower pressure ratio systems. There is very little effect of fuel properties on the efficiency of the F100 sector burner at the idle operating condition. The combustor pressure and inlet air temperature as well as the air-blast fuel nozzles contribute to good fuel preparation and high combustion efficiencies at idle. Over the range of vaporization indexes for the fuels tested with this combustor (Tables 2 and 3), there is but a one-point decrease in idle efficiency attributed to fuel properties. However, for the lower pressure ratio TF33 combustor, there is a significant decrease in combustion efficiency at idle with fuel properties. Over the range of vaporization indexes corresponding to the fuels tested (Tables 2 and 3), the idle efficiency was observed to change by seven points. The effect of fuel property variations on preparation of the fuel air mixtures is significant. It is interesting to note that the correlation obtained for the J79 combustor can is essentially identical to that obtained for the TF33 can, even though the fuel blends evaluated in each were different. The fact that the results shown in Figure 18, for the J79 and TF33 were so similar indicates that the processes controlling mixture preparation and reaction in each were essentially identical and predictable through the use of the vaporization index.

(f) SMOKE

During the performance tests, the smoke number of the exhaust gas discharged from the combustor rigs was measured in accordance with the method described in Reference 14. Of the fuel properties and relationships examined for correlating the smoke numbers, the single variable hydrogen content of the fuel provided the best correlation.

The absolute values of smoke number that were measured in the performance rigs can be quite different from those that might be obtained during engine testing. Experience gained during engine development has shown this to be true. However, rig data is very valuable for providing information on relative changes and in indicating trends. Therefore, the smoke data obtained during the fuel-effects programs for the F100, TF33, and TF30 combustor rigs (References 3-6), as well as the data reported for the J79, F101, and TF41 combustor rigs (References 10-13), were operated on and are presented in Figure 19 in a form showing the tendencies of the different combustor rigs to produce smoke as fuel quality is reduced. In combination with actual engine smoke data, Figure 19 can also be used to estimate the increase in engine smoke number resulting from the use of poorer quality fuels.

To develop Figure 19, the smoke data for the different combustor rigs, operating at simulated sea-level takeoff conditions where smoke production is greatest, were first linearized against the hydrogen content of the fuel used. The smoke numbers measured when the various fuels were burned in a given rig were normalized with the smoke number that was obtained when a referee fuel was burned. The referee fuel selected for developing Figure 19, for all combustors except the TF30, was military-specification JP-4 fuel that contained 14.5 percent hydrogen. For the TF30 combustor, the procedure was somewhat modified because the referee fuel used was military-specification JP-5 that had a hydrogen content of only 13.79 percent. In this case, the linear relationship between smoke number and hydrogen content was extrapolated to a hydrogen content of 14.5 percent, and the smoke number corresponding to this value was used as the normalizing base for the TF30 rig results.

As shown in Figure 19, the rate of increase in smoke number with decreasing hydrogen content is essentially the same for the TF41, TF33, F100, and F101 rigs. However, the rates for the TF30 and J79 rigs are more than twice as great. These trends are the result of the different design features that have been incorporated into the combustors.

6. REFERENCES

1. Bryce Poe II, "Proceedings of the Air Force-Sponsored Industry-Military Energy Symposium", San Antonio, TX, 21-23 October 1980, p. 7

2. W.N. Thorp, "Air Force Fuel Savings," National Defense, December 1982, p. 41

3. J.R. Herrin, "Influence of Shale Oil Base JP-5 on a TF30 Combustor", NAPC-PE-59C, November 1981

4. P.L. Russell, "Fuel Mainburner/Turbine Effects", AFWAL-TR-81-2081, September 1982

5. G.W. Beal, "Effect of Fuel Composition on Navy Aircraft Engine Hot Section Components", NAPC-PE-74C, May 1983

6. J.R. Herrin, et al, "Alternate Test Procedures for Navy Aircraft Fuels-Phase I", NAPC-PE-63C, January 1982

7. D.R. Ballal and A.H. Lefebvre, "Ignition and Flame Quenching of Flowing Heterogeneous Fuel-Air Mixtures", Combustion and Flame 35, 1979, pp. 155-168

8. D.W. Bahr, "Comparison Effects on Broadened Property Jet Fuels on Older and Modern J79 Combustors", ASME Paper 83-6T-81, 1981

9. C.C. Gleason and D.W. Bahr, "Fuel Property Effects on Life Characteristics of Aircraft Turbine Engine Combustors", ASME Paper 80-GT-55, 1980

10. C.C. Gleason, et al,"Evaluation of Fuel Character Effects on J79 Engine Combustion System", AFAPL-TR-79-2015, April 1979

11. C.C. Gleason, et al, "Evaluation of Fuel Character Effects on F101 Combustion System", AFAPL-TR-79-2018, June 1979

12. C.C. Gleason, et al, "Evaluation of Fuel Character Effects on J79 Smokeless Combustor", AFWAL-TR-80-2092, November 1980

13. R.E. Vogel, et al, "Fuel Character Effects on Current High Pressure Ratio, Can Type Combustion Systems", AFAPL-TR-79-2072, April 1980

14. SAE Aerospace Recommended Practice 1179A, "Aircraft Gas Turbine Engine Exhaust Smoke Measurement", Society of Automotive Engineers, New York, N.Y., July 16, 1979

15. J. Emory, et al, "Effect of Gas Turbine Fuel Nozzle Design and Operation on Nozzle and Combustor Performance", P&WA Report PWA-3751 to the Naval Air Engineering Center, 1969

16. M.S.M.R. El Shanawany and A.H. Lefebvre, "Airblast Atomization", Prog. Energy Comb. Sci. 6, 1980, pp. 233-261

7. ACKNOWLEDGEMENT

The author wishes to acknowledge the support of the United States Air Force and Navy in sponsoring the alternative-fuel and fuel-effects programs from which this paper is derived. He would like to specifically thank Tom Jackson and Chuck Delaney of the Air Force's Wright Aeronautical Laboratories; and Buck Nowack and Pete Karpovich of the Navy's Air Propulsion Center for their technical and managerial contributions, and for their patience.

The author also wishes to acknowledge the valuable contributions of his collegues in fuel-effects technology at Pratt & Whitney Aircraft. These include John Herrin, Art Masters, Paul Russell, Rich Ernst, Tom Rolfe, George Beal and Dean Andreadis.

8. APPENDIX

Vaporization Index (VI)

The vaporization index (VI) is defined in equation (1') as

$$VI = \frac{(RDS)^2(SG)}{\log (1 + B)} \qquad (1')$$

and contains the three principal variables relative droplet size (RDS), specific gravity (SG), and mass-transfer number (B).

The relative droplet size, is defined in equation (2') as

$$RDS = \frac{SMD}{(SMD)_{reference}} \qquad (2')$$

and is the ratio of the Sauter mean diameter of a fuel obtained under a given set of operating conditions. For pressure-atomizing fuel injectors, for example, relative drop size has been estimated using relationships from Reference (16), which has been simplified to the expression shown in equation (3')

$$\left[\frac{\sigma}{\sigma_{ref}}\right]^{0.6} = \left[\frac{\nu}{\nu_{ref}}\right]^{0.2} \qquad (3')$$

where σ = surface tension
ν = kinematic viscosity
ref = reference

Similar relationships can be developed for air-blast fuel injectors (Reference 17).

The mass-transfer number (B) is defined in equation (4') as

$$B = \frac{(m_{o,g} H/r) + c (T_g - T_s)}{Q} \qquad (4')$$

where $m_{o,g}$ = mass fraction of oxygen

H = heat of combustion

r = stoichiometric ratio

c = specific heat at constant pressure

T_g = combustor inlet temperature

T_s = recovery temperature; 10% recovery point for ignition and 90% recovery point for combustor efficiency and pattern factor

Q = heat conducted from gas per unit mass crossing the phase boundary, as defined in equations (5') and (6') which is the sum of the latent heat of vaporization and the increase in enthalpy between the base temperature and the surface temperature

$$Q = L + c_l (T_s - T_o) \tag{5'}$$

$$Q = L_o + c_{vap} (T_s - T_o), \tag{6'}$$

where L = latent heat of vaporization at droplet surface

c_l = specific heat or liquid

T_s = surface temperature of liquid

c_{vap} = specific heat of vapor at constant pressure

L_o = latent heat of vaporization at T_o

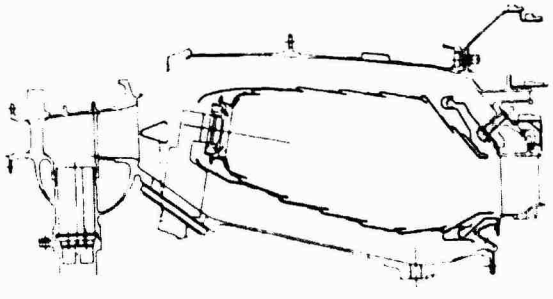

Figure 1. F100 Combustion Section Flow Path

Figure 2. Instrumented TF33 Combustor Can

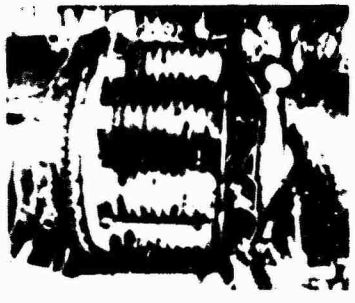

Figure 3. TF30 Can-Annular Ignition Rig

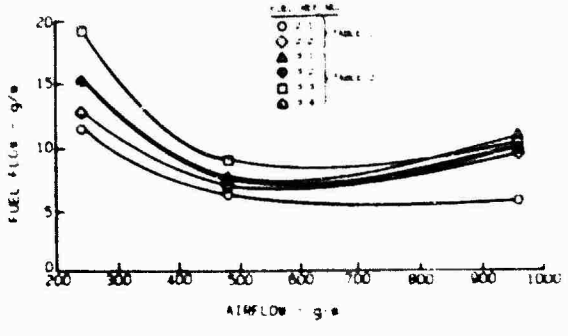

Figure 4. Cold Day (244K) Groundstart Ignition Characteristics for the F100 Sector Burner Rig

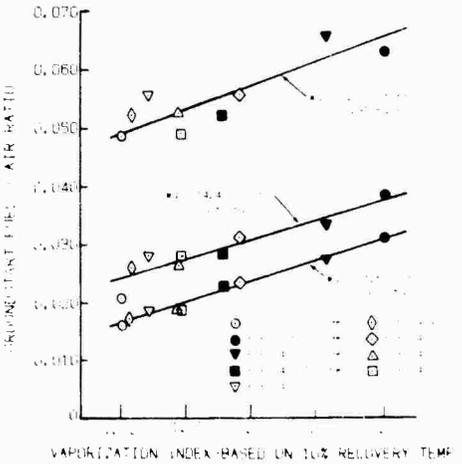

Figure 5. Groundstart Ignition Characteristics for the TF30 Combustor Rig

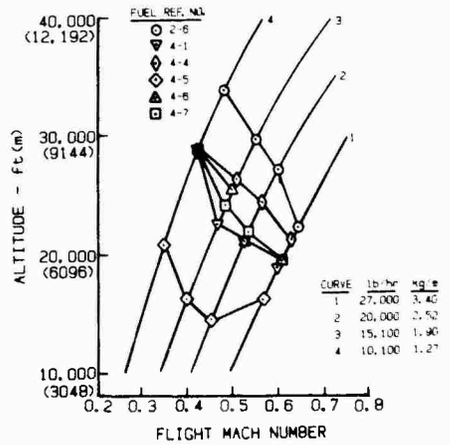

Figure 6. Fuel Effects on Airstart Ignition for Ignition Rig

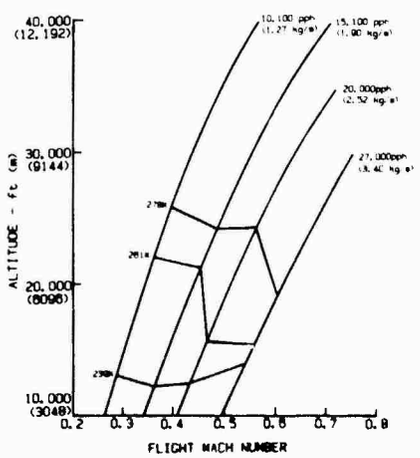

Figure 7. Temperature Effects on Airstart Ignition for TF30 Ignition Rig Using JP-5 Fuel (Fuel No. 2-5)

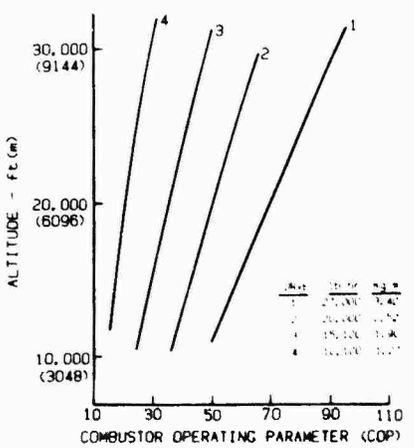

Figure 8. Effect of Altitude on Combustor Operating Parameter for TF30 Ignition Rig

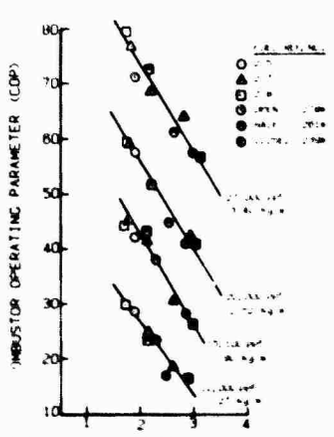

Figure 9. Variation in Combustor Operating Parameter with Fuel Characterization Parameter for TF30 Ignition Rig

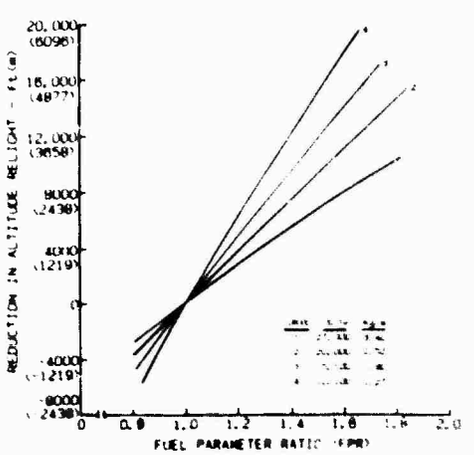

Figure 10. General Variation in Airstart Relight Altitude with Fuel Parameter Ratio for TF30 Ignition Rig

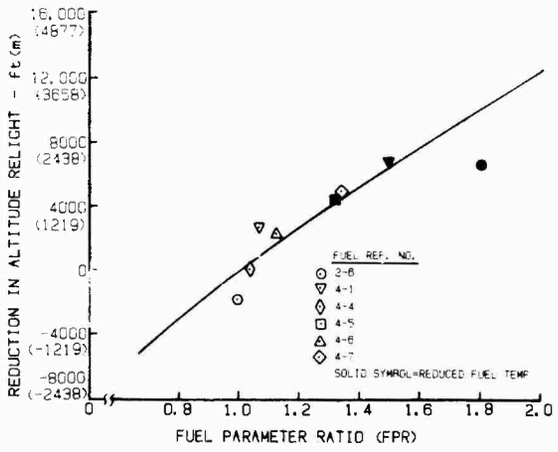

Figure 11. Specific Variation in Airstart Relight Altitude with Fuel Parameter Ratio for TF30 Ignition Rig

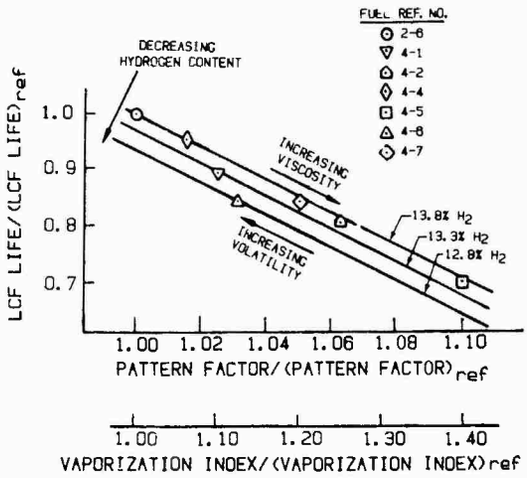

Figure 12. Predicted Fuel Effect On LCF Life for TF30 First Turbine Vane

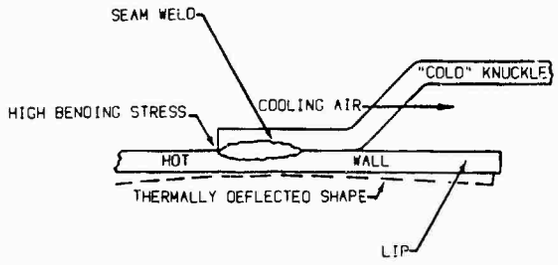

Figure 13. Thermal Stress Model

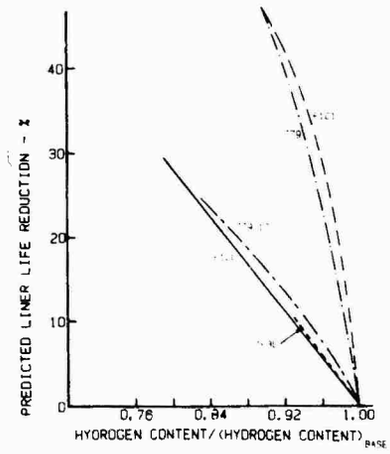

Figure 14. Predicted Liner Life Reduction

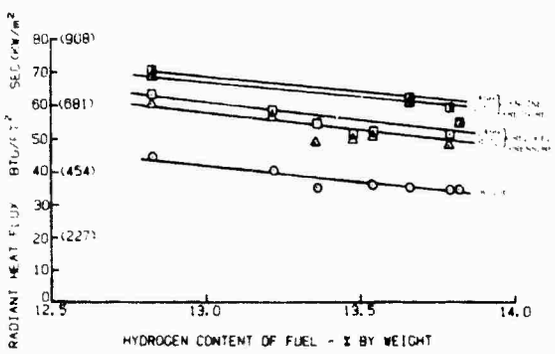

Figure 15. Measured Variation in Thermal Radiation Rate in TF30 Combustor Rig

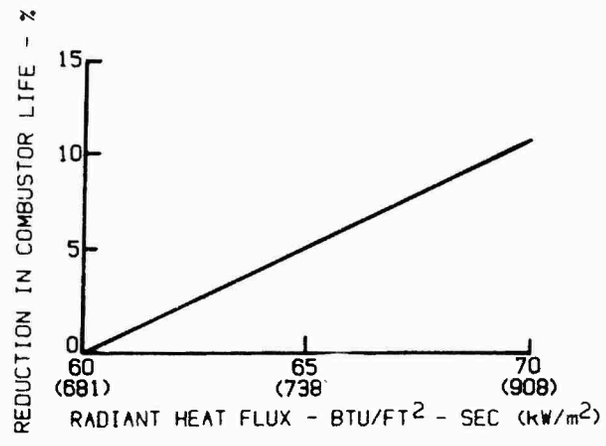

Figure 16. Reduction in Predicted Liner Life for TF30 Combustor Rig Due to Thermal Radiation

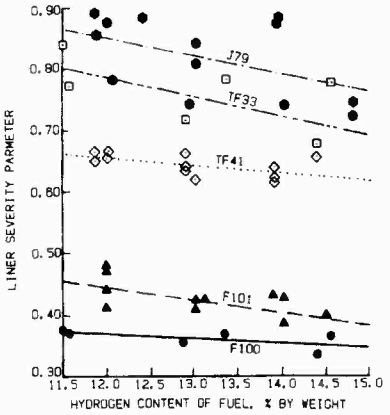

Figure 17. Variation in Liner Severity Parameter With Hydrogen Content of Fuel

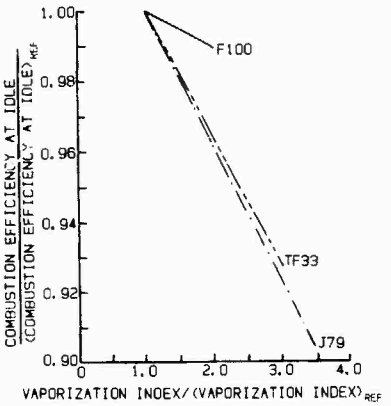

Figure 18. Variation in Combustor Efficiency at Idle With Vaporization Index

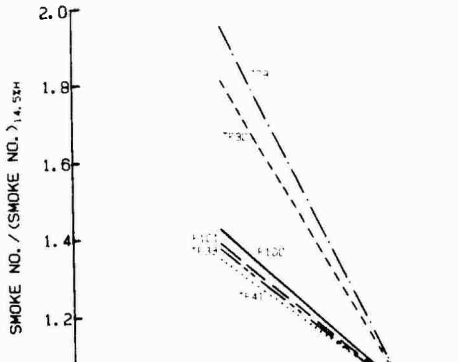

Figure 19. Variation in Smoke Number at Sea-Level Takeoff with Hydrogen Content

DISCUSSION

J.Vleghert

You mentioned effects of fuel temperature on several characteristics of combustion; is there also an influence on smoke production?

Author's Reply

An increase in the temperature of a fuel that is injected into a combustion chamber should, in general, serve to produce a lower level of smoke in the exhaust gas. The elevated temperature, in essence, increases the volatility of the fuel. Enhanced volatility has been demonstrated to assist in the suppression of smoke and carbon deposition.

C.Moses, US

You have had considerable success in developing a parameter for fuel properties for use in correlating engine performance characteristics. Have you done any work in trying to include engine design characteristics so that many engines can be correlated together into one model?

Author's Reply

We have been successful in correlating characteristics of specific engine burners using the parameters described in the paper. We have not yet developed a unified parameter that would apply to a wide range of gas turbine engine burners.

J.Peters, US

In regard to the question of extending your correlations (particularly for ignition) of fuel effects to include different engines, I believe it can be done by including air mass flow rates and geometry with reference velocity and fuel injector effects with drop size correlations. This is illustrated for ignition, lean blowoff and combustion efficiency in Paper No.32

G.Winterfeld, Ge

The two parameters used, vaporization index VI and fuel characterization parameter, FPC, look quite similar, with the exception of the exponent of drop size. Can you comment on that difference in the two parameters?

Author's Reply

The fuel characterization parameter FCP, defined in equation (3), was formulated for predicting altitude ignition characteristics from the quenching distance relationship of Lefebvre and Ballal (reference 7). The value of $(SMD)^{1.5}$, which appears in their basic equation, has been maintained per se. The vaporization index VI, as defined in equation (1), was developed for groundstart ignition, combustion efficiency, pattern factor and lean blowout from a relationship relating droplet lifetime to the square of the droplet diameter. In the derivation, the single droplet diameter term was replaced with SMD for a droplet array and was normalized using the value of SMD for a reference fuel. Therefore, the expression for VI includes an SMD ratio rather than an absolute value (as in the expression for FCP), and the exponent of the ratio has been maintained as a square term. The exponential difference between 1.5 and 2 is small; however, the terms being raised to the different powers are quite different.